Solar Phys (2019) 294:70
https://doi.org/10.1007/s11207-019-1461-3

An Extended Study of the Precursory Signs of Forbush Decreases: New Findings over the Years 2008 – 2016

D. Lingri[1] · H. Mavromichalaki[1] · A. Belov[2] · M. Abunina[2] · E. Eroshenko[2] · A. Abunin[2,3]

Received: 1 February 2019 / Accepted: 16 May 2019 / Published online: 5 June 2019

Abstract In spite of the fact that the current Solar Cycle 24 is close to its end now, it is a less active Solar Cycle, during its time period (2008 – 2016) and a lot of Forbush decreases of cosmic ray intensity with rigidity 10 GV and amplitude greater than 2% were recorded by the ground-based neutron monitors. Among these events, the ones associated with sudden geomagnetic storm commencements (SSCs) and presenting a first harmonic of cosmic ray anisotropy greater than 0.8% were examined. Cosmic ray data recorded at the neutron monitor stations were obtained from the European high resolution neutron monitor database, while the Forbush decreases, accompanied by their characteristics were accessed from the updated Database of the *Institute of Terrestrial Magnetism, Ionosphere and Radio Wave Propagation* (IZMIRAN). Solar, interplanetary and geomagnetic characteristic parameters of each event separately have been studied in detail and analyzed. It was shown through the usage of the "ring of neutron monitor stations" method that, in some cases, precursory signals before the main phase of the event appeared. After an extended study of the Forbush decreases precursors during the examined period, the appearance of pre-decreases and/or pre-increases of the cosmic ray intensity before the beginning of the events, acting as precursory signals, were identified in almost half of the cases studied. In combination with other parameters, their common features are discussed, with the purpose of monitoring and possibly forecasting the space-weather conditions.

Keywords Forbush decreases · Cosmic ray intensity · Precursors · Neutron monitors

✉ H. Mavromichalaki
emavromi@phys.uoa.gr

1 Faculty of Physics, National and Kapodistrian University of Athens, Athens, Greece

2 Pushkov Institute of Terrestrial Magnetism, Ionosphere and Radio Wave Propagation (IZMIRAN) of the Russian Academy of Sciences, Moscow, Russia

3 Kalmyk State University, Elista, Russia

1. Introduction

Sudden disturbances originating from the Sun, such as coronal mass ejections (CMEs), high speed solar wind streams, *etc*., interact with the galactic cosmic rays (CRs) in the interplanetary medium and arrive at the Earth earlier than the main perturbation. As a result, sudden storm commencements (SSCs) are created in the magnetosphere and decreases are observed in the CR intensity (Forbush, 1954), known as "sporadic" Forbush decreases (FDs) recorded at the neutron monitors (NMs) (Lockwood, 1971; Cane, 2000; Belov, 2009; Belov *et al.*, 2014).

The term "sporadic" FD describes FDs which are connected with interplanetary coronal mass ejections (ICMEs) that are the interplanetary counterparts of the solar CMEs, and in most cases cause SSCs (Gopalswamy *et al.*, 2001; Paouris and Mavromichalaki, 2017). The sporadic FDs are characterized by an asymmetric shape, which is large, sharp, deep and the initial phase lasts no more than one day, as a rule, while the recovery phase lasts usually longer (Cane, 2000; Mavromichalaki *et al.*, 2005; Lingri *et al.*, 2016a; Melkumyan *et al.*, 2019 and references therein). Another kind of FDs is the "recurrent" ones, which are smaller, smoother and more symmetrical than the sporadic ones. They are produced by high speed solar wind streams originating from coronal holes (Abunin *et al.*, 2012; Dumbovic *et al.*, 2012; Gerontidou, Mavromichalaki, and Daglis, 2018) and seldom are associated with SSCs. In general, in the most cases the FDs are associated with geomagnetic disturbances, storms or sub-storms, due to their common sources (Belov, 2009; Aslam and Badruddin, 2017).

Around the start of a FD, characteristic changes in the CR intensity such as pre-decreases and pre-increases, as well as changes in the first harmonic of the anisotropy at the ecliptic plane may appear some hours before the start of the event and can be useful for forecasting the upcoming disturbance (Belov *et al.*, 1995; Munakata *et al.*, 2005; Papailiou *et al.*, 2012a, 2012b; Tortermpun, Ruffolo, and Bieber, 2018). They can be observed from 20 h up to 1 – 2 h earlier than the start of the main phase of the Forbush decrease, which in most cases is important for the early detection of the event (Nagashima *et al.*, 1993; Leerungnavarat, Ruffolo, and Bieber, 2003; Asipenka *et al.*, 2009).

These changes of the FDs that can act as precursory signals originate from the response of the CR to the approaching shock and they tend to have a distinct direction and time distribution (Belov *et al.*, 1995; Papailiou *et al.*, 2012a, 2012b). Especially, viewing directions for which the detected cosmic rays have come from downstream of the shock, where there is a lower cosmic ray density, known as the "loss cone" effect, creates a pre-decrease (Belov *et al.*, 1995; Leerungnavarat, Ruffolo, and Bieber, 2003). On the other hand, the CR particles reflected by the front of the shock are accelerated and recorded at the Earth as pre-increases (Dorman *et al.*, 1995). The observed precursor sign for each event depends on the heliographic position of the solar source in combination with the Earth's position in the heliosphere (Kozai *et al.*, 2016).

According to Papailiou *et al.* (2012a) and Tortermpun, Ruffolo, and Bieber (2018) the precursors of the FDs appear with their pitch angle depending on the CR intensity. This cannot be described only by the first two CR harmonics of anisotropy. These CR intensity anomalies can be detected by applying data analysis of the neutron monitors of the worldwide network as well as by analyzing data of the global muon detector network (Munakata *et al.*, 2005; Fushishita *et al.*, 2010 and references therein). In this study we will focus on the NM data as their network extends all over the world and records high energy particles (http://www.nmdb.eu/; Mavromichalaki *et al.*, 2011).

CR anisotropy is based on interplanetary magnetic field (IMF) variables, such as density, direction, and degree of regularity, on solar wind (SW) velocity and on CR density gradient.

The CR anisotropy (A_{xy}) component on the equatorial plane is close to the solar diurnal anisotropy, while NM measurements have the opportunity to distinguish the CR anisotropy. Moreover, the first harmonic of the CR anisotropy is also increasing hours prior to the SSC's arrival and the vector's direction changes significantly (Belov *et al.*, 2017a). The changes of the precursor detection are connected to the features of the interplanetary disturbances and to the solar and interplanetary parameters, such as solar wind and IMF, as well as to the source location on the solar disc (Belov *et al.*, 2017b).

It is crucial to study the first harmonic of the CR anisotropy on the equatorial plane (A_{xy}) some hours before the SSC. As is well known, a typical steady anisotropy of cosmic rays exists with an amplitude of $A_{xy} = 0.51 - 0.53\%$ for a stable solar wind, independently of the SW velocity (Belov *et al.*, 2017a). If a number of large enough changes occur in the solar wind (increasing velocity, changes in A_0 or strengthening of IMF) the value of the A_{xy} component increases significantly, especially under growing IMF or large changes of the CR density. In previous work, the criterion for the A_{xy} anisotropy before the event was taken to be greater than 1.2% (Papailiou *et al.*, 2012a; Papailiou *et al.*, 2012b), which is by far greater than the steady value. An extensive study in this field showed that the criterion of A_{xy} anisotropy would be considered as much lower than this value, closer to that of 0.8%. In this way, more events that present warning signals are revealed.

In this work a reviewing study of the criteria that were used till now for the determination of precursory signs at the beginning of the Forbush decreases of cosmic ray intensity, is presented. FD events for cosmic rays of 10 GV rigidity characterized by amplitude greater than 2% observed during the Solar Cycle 24, over the years 2008 – 2016, and associated with interplanetary disturbances causing SSC, were selected. The ecliptic component A_{xy} of the cosmic ray anisotropy before the start of the FD was chosen to be greater than 0.8% and the interplanetary space conditions to be quite undisturbed. In Section 2 the data sources as well as the selection procedure are presented. In Section 3 various characteristic precursory events have been categorized and are presented and finally Section 4 contains a discussion and new conclusions of this study.

2. Data Analysis

The Solar Cycle 24 is considered as a very low activity Solar Cycle without severe solar events that could lead to great FDs in the CR intensity recorded at the Earth's surface (Ross and Chaplin, 2019). This cycle started on December 2008, reached a maximum on June 2014 and it is the lowest Solar Cycle since the Dalton minimum, recorded around the year 1810 (https://nextgrandminimum.com/2019/01/31/Solar-Cycle-24-has-had-the-lowest-solar-activity-since-the-dalton-minimum-around-1810/). Monthly values of the cosmic ray intensity as recorded by Oulu neutron monitor station (http://www.nmdb.eu/nest/) and of the solar activity expressed by the sunspot number (R_z) at the link http://www.sidc.be/silso/datafiles #total for the considered time period from January 2008 to December 2016 are presented in the upper and middle panels of Figure 1, respectively. This time period covers the extended minimum between the Solar Cycles 23 and 24, the ascending, the maximum and most of the descending phases of the Solar Cycle 24. The well-known anti-correlation of these two parameters due to the 11-year solar modulation, regarding the low solar activity in contrast to the high cosmic ray intensity and *vice versa*, is clearly visualized in the upper panel of Figure 1 (Forbush, 1954).

In this work, the Forbush decrease database, known as *Forbush Effects* and *Interplanetary Disturbances database* (FEID), created by the cosmic ray group of the *Institute of Terrestrial*

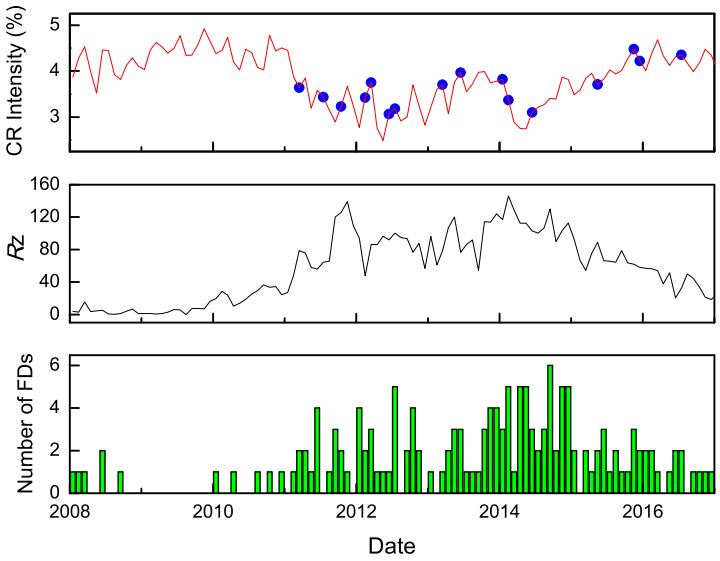

Figure 1 Time profiles of the normalized cosmic ray intensity of 10 GV (*upper panel*) and of the sunspot number (*middle panel*). The *purple circles* in the *upper panel* indicate the events associated with precursors of all categories. The number of the recorded FDs with amplitude greater than 2% during the time period 2008 – 2017 is presented in the *lower panel*.

Magnetism, Ionosphere and Radio Wave Propagation (IZMIRAN) of Russian Academy of Sciences in collaboration with the cosmic ray group of the Physics Faculty of the *National and Kapodistrian University of Athens* was used (http://spaceweather.izmiran.ru/eng/dbs.html). This database includes all the FDs, accompanied by their characteristics, as recorded by the worldwide neutron monitor network from the beginning of their operation till now (1957 – 2017). It is noted that in this database the cosmic ray intensity with a rigidity of 10 GV at the top of the atmosphere and magnetosphere was obtained by all the neutron monitor stations by using the *Global Survey Method* (GSM) (Belov *et al.*, 2018).

Moreover, data regarding the solar flares used in this work have been obtained from NOAA, by using data collected by the *Geostationary Operational Environmental Satellites* (GOES) (https://www.ngdc.noaa.gov/stp/space-weather/solar-data/solar-features/solar-flares/x-rays/goes/xrs/). Other solar data such as active regions and CMEs have been retrieved from the website https://www.spaceweatherlive.com/en/archive/ and from the *Solar and Hemispheric Observatory* (SOHO) and especially from its *Large Angle and Spectrometric Coronagraph* (LASCO), known as the SOHO/LASCO Catalog (https://cdaw.gsfc.nasa.gov/CME_list/), respectively. The ICMEs data are obtained from the Richardson and Cane ICMEs list (http://www.srl.caltech.edu/ACE/ASC/DATA/level3/icmetable2.htm), and the interplanetary and geomagnetic parameters such as Kp, Dst, IMF, SSC, *etc*. are obtained from the OMNIWeb site (https://omniweb.gsfc.nasa.gov/). Cosmic ray intensity data of high resolution (1 min and 1 h) are accessed from the neutron monitor database-NMDB (www.nmdb.eu), which provides data from all the operating neutron monitors.

From a total of 1010 events that are recorded in the FEID database during the examined time interval 2008 – 2016, only 142 have amplitude greater than 2% (Figure 1; lower panel). This means that the examined period was indeed of low solar activity. It is of interest to note that in the previous Solar Cycles the average number of FDs was 6 to 10% greater than

those of the Solar Cycle 24. After a detailed study of these events and taking into account the special preconditions of this cycle we were led to the following specific criteria for the study of the possible precursors of the FDs:

i) The amplitude of the selected FDs recorded at the neutron monitors was defined to be equal to or greater than 2% for the cosmic rays of 10 GV rigidity obtained by the Global Survey Method (Belov *et al.*, 2018). This cosmic ray time series is representative outside the atmosphere and magnetosphere to all neutron monitor measurements provided by the worldwide network. This amplitude has been chosen in order to avoid the loss of FDs with observable precursor signals as well as not to be confused with the cosmic ray intensity's background.

ii) The FDs were associated with a sudden geomagnetic storm commencement (SSC).

iii) The anisotropy of cosmic rays of 10 GV at the ecliptic plane before the shock's arrival was defined to be greater than 0.8%. The mean value of this cosmic ray anisotropy component is usually smaller than 0.6% (Belov, 2009; Papailiou *et al.*, 2012a) and the amplitude of the precursory pre-decreases/pre-increases is about 2σ. The adopted value of A_{xy} component is considered to be $> 0.8\%$ in order to avoid loss of possible precursors of FDs. T he value of 10 GV rigidity is close to the effective rigidity of the neutron monitors with the highest latitude and the calculated A_{xy} values are close to the amplitudes of the diurnal variation of these neutron monitors (sub-polar stations are excluded) (Belov *et al.*, 2017a).

After a detailed study of the 1010 events was performed during the considered time window (2008 – 2016), a number of 34 FDs were found to obey the above criteria. From them, only those in which the CR intensity and the interplanetary space before the studied FD were undisturbed for about one or two days before were selected for analysis. The final dataset included a number of 16 FDs suitable for further study. Each one of them is indicated in the middle panel (blue dots) of Figure 1, while they are described in more detail in Table 1.

This table consists of 15 columns. The first column provides the number of each event; the second one contains the date and the time when the shock reached the Earth and the third one provides the FD magnitude at the rigidity of 10 GV. The next two columns contain the characteristic values of the geomagnetic indices Kp and Dst for the same time period. From the sixth to the eighth the maximum value of the interplanetary magnetic field, the maximum solar wind velocity and the maximum value of the anisotropy at the ecliptic plane are presented, respectively. The following four columns are mentioned on the characteristic solar parameters of the event, as the type of flare, the date and time that it was observed on Sun, the exact coordinates of it on the solar disc and the number of its active region. Finally, the last three columns present the CME related to the flare, when it was recorded from the SOHO/LASCO coronagraph, its maximum velocity and the CME's type, respectively.

For the study of the precursory signs of the FDs the asymptotic longitudinal cosmic ray distribution diagrams for each examined event were plotted using the "Ring of Stations" method (Belov *et al.*, 2003; Asipenka *et al.*, 2009; Papailiou *et al.*, 2012a). Hourly corrected for pressure data recorded at 22 selected NMs of the worldwide network, were used by this method (Table 2). These stations were chosen with cut-off rigidities smaller than 3 GV and located at altitude smaller than 1000 m, as their data have great sensitivity to CR anisotropy and similar sensitivity to density variations. The sub-polar NMs stations that show high sensitivity to the north–south anisotropy (A_z) were also excluded. This is really helpful because of the anisotropic characteristic of the precursors and of the FDs in general (Belov *et al.*, 2017a, 2017b). The asymptotic directions of these stations were calculated using the Tsyganenko96 model from the cut-off rigidity of each station up to 999 GV (Tsyganenko and Stern, 1996; Plainaki *et al.*, 2009).

Table 1 The studied FDs with precursors of the current Solar Cycle are presented. The events with a superscript star are associated with a pre-decrease precursor, those with a superscript × are associated with a pre-increase precursor and the others are connected with both signs.

A/A	SC date time DD.MM.YYYY hh:mm (UT)	FD ampl. (%)	Kp max	Dst min (nT)	B_{imf} (nT)	V_{max} (km s^{-1})	A_{xy}	Flare (≥ C)	Flare date time DD.MM.YYYY hh:mm (UT)	Source	Active region	CME date time DD.MM.YYYY hh:mm (UT)	V_{CME} (km s^{-1})	CME type
1	10.03.2011 06:45	2.5	5.3	−83	11.9	405	3.00	M3.7	07.03.2011 19:43	N24W46	AR 11164	07.03.2011 20:00	2125	halo
2*	11.07.2011 08:50	3.2	3.7	−28	12.6	708	1.69	B4.7	08.07.2011 23:57	S17E20	AR11247	09.07.2011 00:48	630	partial halo
3	24.10.2011 18:31	4.9	7.3	−147	24.0	534	1.95	–	–	–	–	22.10.2011 01:25	593	halo
4*	26.02.2012 21:39	3.5	5.3	−57	14.9	493	2.14	–	24.02.2012 02:25	N32E38	–	24.02.2012 03:46	800	partial halo
5×	12.03.2012 09:14	5.7	6.3	−51	23.6	727	3.27	M8.4	10.03.2012 17:15	N18W13	AR 11429	10.03.2012 18:00	1296	halo
6*	16.06.2012 20:19	4.6	6.3	−86	40.1	519	1.90	M1.9	14.06.2012 12:52	S17E06	AR 11504	14.06.2012 14:12	987	halo
7	14.07.2012 18:09	6.4	7.0	−139	27.3	667	2.62	X1.4	12.07.2012 15:37	N13W15	AR 11522	12.07.2012 16:48	885	halo
8*	17.03.2013 05:59	4.6	6.7	−132	17.8	725	1.72	M1.1	15.03.2013 05:46	N07E07	AR 11692	15.03.2013 07:12	1063	halo
9×	23.06.2013 04:26	5.9	4.3	−49	7.6	697	1.70	M2.9	21.06.2013 02:30	S16E73	AR 11777	21.06.2013 03:12	1900	partial halo
10×	07.01.2014 15:12	4.3	3.3	−22	8.1	440	1.50	M4.0	04.01.2014 19:05	S09E53	AR 11944	04.01.2014 21:22	977	halo
11	15.02.2014 13:16	4.0	5.0	−37	16.2	450	1.96	M2.1	12.02.2014 15:41	S12E03	AR 11974	12.02.2014 16:36	533	halo
12	07.06.2014 16:52	4.7	6.3	−37	26.0	616	2.93	–	–	–	–	04.06.2014 12:48	467	halo
13*	06.05.2015 01:42	3.2	5.3	−28	17.5	479	1.88	–	–	–	–	02.05.2015 20:24	335	halo
14×	06.11.2015 18:18	3.2	6.0	−96	19.4	677	2.23	M3.7	04.11.2015 13:31	N09W04	AR 12443	04.11.2015 14:48	578	halo
15	31.12.2015 00:50	4.8	6.0	−110	16.9	485	2.57	M1.8	28.12.2015 11:20	S22W05	AR 12473	28.12.2015 12:12	1212	halo
16×	19.07.2016 23:51	2.9	5.0	−23	27.3	576	2.03	C1.4	17.07.2016 05:36	N07E14	AR 12567	17.07.2016 10:48	340	halo

Table 2 The neutron monitor stations and their characteristic parameters used in this work.

A/A	NMDB stations	Abbr.	Geograph. coordinates	Rigidity (GV)	Altitude (m)
1	Apatity, Russia	APTY	67.57°N 33.40°E	0.65	177
2	Barentsburg, Russia	BRBG	78.06°N 14.22°E	0.00	51
3	Cape Shmidt, Russia	CAPS	68.92°N 179.47°W	0.45	0
4	Fort Smith, Canada	FSMT	60.02°N 111.93°W	0.30	180
5	Inuvik, Canada	INVK	68.36°N 133.72°W	0.30	21
6	Kerguelen, France	KERG	49.35°S 70.25°E	1.14	33
7	Kingston, Australia	KGSN	42.99°S 147.29°E	1.88	65
8	Kiel, Germany	KIEL	54.34°N 10.12°E	2.36	54
9	Magadan, Russia	MGDN	60.04°N 151.05°E	2.10	220
10	Moscow, Russia	MOSC	55.47°N 37.32°E	2.43	200
11	Mirny, Antarctica	MRNY	66.55°S 93.02°E	0.03	30
12	Mawson, Antarctica	MWSN	67.60°S 62.88°E	0.22	0
13	Nain, Canada	NAIN	56.55°N 61.68°W	0.30	46
14	Newark, USA	NEWK	39.68°N 75.75°W	2.40	50
15	Norilsk, Russia	NRLK	69.26°N 88.05°E	0.63	0
16	Novosibirsk, Russia	NVBK	54.48°N 83.00°E	2.91	163
17	Oulu, Finland	OULU	65.05°N 25.47°E	0.81	15
18	Peawanuk, Canada	PWNK	54.98°N 85.44°W	0.30	53
19	Sanae IV, Antarctica	SNAE	71.40°S 02.51°W	0.73	856
20	Terre Adelie, Antarctica	TERA	66.65°S 140.00°E	0.00	32
21	Tixie Bay, Russia	TXBY	71.01°N 128.54°E	0.48	0
22	Yakutsk, Russia	YKTK	62.01°N 129.43°E	1.65	105

3. Selected Events

After an analytical study of the aforementioned events listed in Table 1 by using the tools described in the previous section and especially the asymptotic longitudinal diagrams, it is mentioned that in the selected FDs, either pre-increase or pre-decrease signs and in some cases both of them were observed. These events can be separated into three categories and typical examples of each category are presented below.

3.1. Forbush Decreases with Pre-decrease Precursors

The first group of the FDs characterized by only pre-decrease signs before the main phase of them includes a number of five events during the examined period. These events are the ones of 11 July 2011, of 26 February 2012, of 16 June 2012, of 17 March 2013 and of 06 May 2015. It is interesting that their characteristics are variable, as the geomagnetic and the interplanetary parameters are changed from event to event. However, the values of all the parameters (like interplanetary magnetic field intensity, geomagnetic indices, *etc*.) for all the examined events were rapidly increased as a result of the incoming SSC.

In particular, during the event of 06 May 2015, a SSC reached the Earth's magnetosphere at 1:42 UT. On 02 May 2015 at 20:24 UT, a halo CME from the Sun with a velocity of 335 $\mathrm{km\,s^{-1}}$ was recorded by the SOHO satellite. It was the first one of a series of halo CMEs that were observed in a two days period. The solar wind velocity peaked at 479 $\mathrm{km\,s^{-1}}$

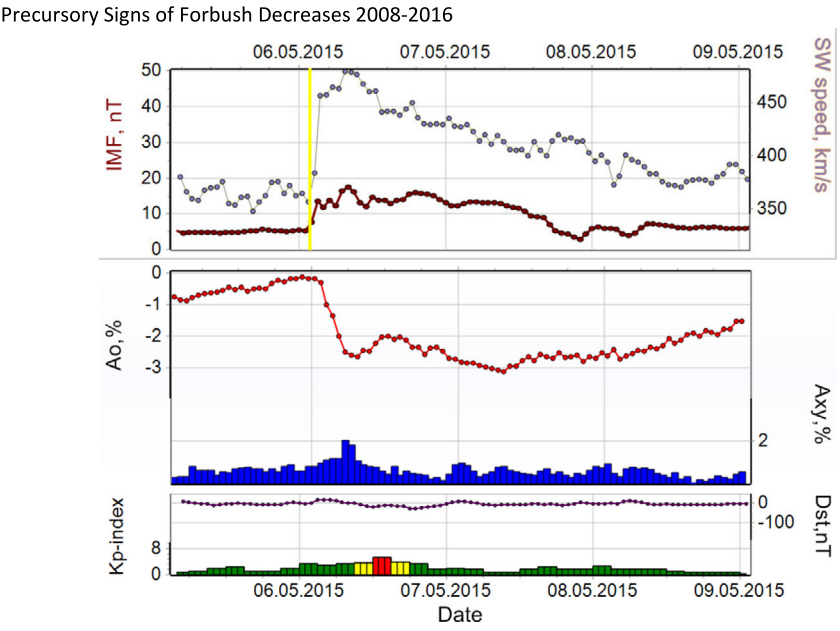

Figure 2 Time profiles of the solar wind velocity (*purple line*) and the interplanetary magnetic field (*red line*) (*upper panel*), of the CR density (A_0) (*red line*) and the anisotropy on the ecliptic plane A_{xy} (*blue histogram*) (*middle panel*) and of the geomagnetic indices Dst and Kp (*line* and *histogram*, respectively) (*lower panel*) for the FD on 6 May 2015.

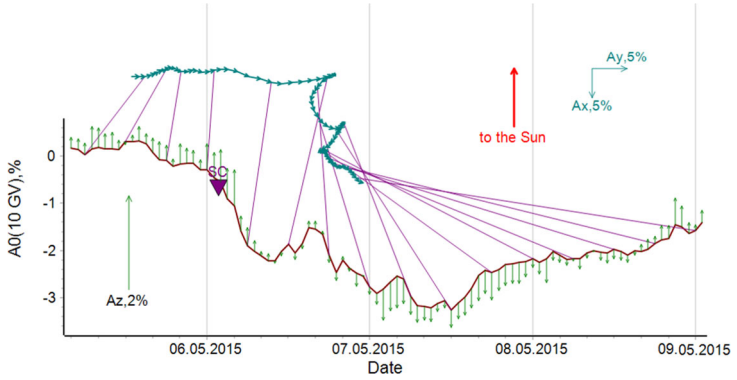

Figure 3 The anisotropy variation on the ecliptic plane (A_{xy} – *blue vectors*) and of the z component (A_z – *green vectors*) during the time period of the event of 06 May 2015. The *red line* represents the A_0 component. *Purple lines* connect the same points in time on two curves.

and the IMF intensity reached the value of 17.5 nT, as it is presented in the upper panel of Figure 2. A FD with a 3.2 % amplitude of the 10 GV cosmic rays was recorded and the solar diurnal anisotropy at the ecliptic plane and its north–south component were increased significantly ($A_{xy} = 1.88\%$, $A_z = 1.44\%$) (Figure 2, middle panel; Figure 3), with simultaneous strong changes in its direction (Figure 3). The geomagnetic indices Kp and Dst reached the values of 5+ and −28 nT, respectively, during the FD (Figure 2, lower panel).

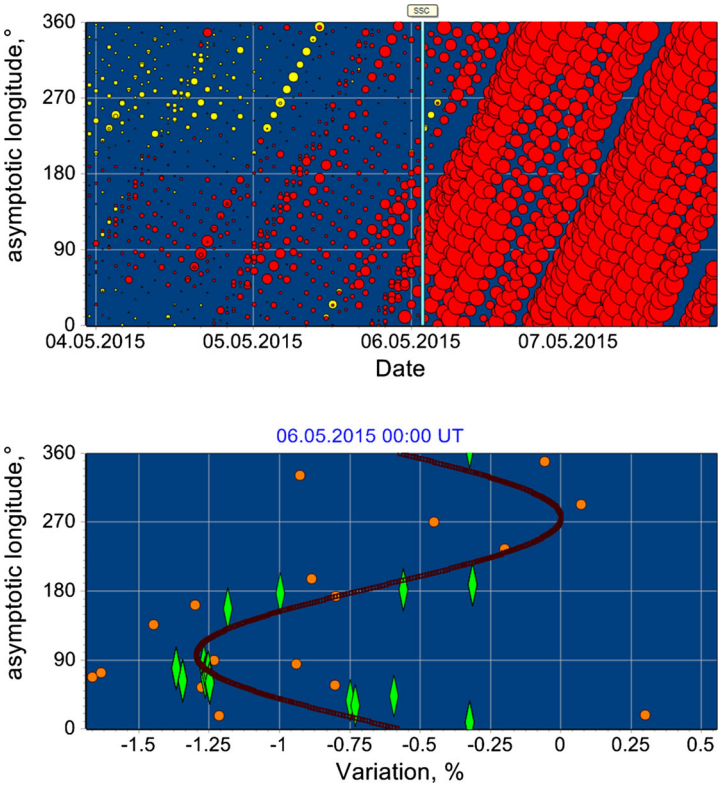

Figure 4 The asymptotic longitude of each station *versus* the date (*upper panel*) for the FD of 6 May 2015. The *red circles* represent decrease in the CR intensity while *yellow* ones represent increase. *Cyan vertical line* is the shock's arrival time. The switching of *yellow* and *red circles* two days before the FD is the solar diurnal anisotropy record. The size of its bubble is proportional to the recorded amplitude of each station every hour. The asymptotic longitude of each station *versus* hourly cosmic ray variations of NMs (*lower panel*) at 00:00 UT on 6 May 2015 (1 h before the FD's onset) is presented. The *orange dots* present the hourly CR variations, the *green diamonds* present CR variations averaged within the sector $\pm 20°$ and the *curve* gives the fitting of the first harmonic of the anisotropy (solar–diurnal variation) calculated from the longitudinal distribution.

In order to examine the existence of any precursor sign in the examined event we sketched the diagrams of the asymptotic longitudinal distribution of CR intensity, using the "Ring of Station Method", presented in the upper panel of Figure 4. The red bubbles indicate the decrease of the CR intensity while the yellow bubbles refer to the CR increase, relatively to an undisturbed base-period before the FD. The cyan line represents the time that the SSC was recorded. The size of each bubble is proportional to the variation range. From the diagram of this event it is obvious that a pre-decrease sign appeared about 16 h before the SSC at an asymptotic longitudinal range between 50° and 170°. One hour before the SSC registration, a significant decrease in the CR intensity at many stations in the longitudinal zone of 70 – 160° was observed (see Figure 4, lower panel). In this diagram the orange dots present the hourly CR variations, the green diamonds present CR variations averaged in the sector $\pm 20°$ and the curve indicates the fitting of the first harmonic of the anisotropy (solar–diurnal variation) calculated from the longitudinal distribution.

To summarize, the asymptotic longitudinal diagrams where the precursor sign is observed, are different for each FD of this group with a common range of the pre-decrease,

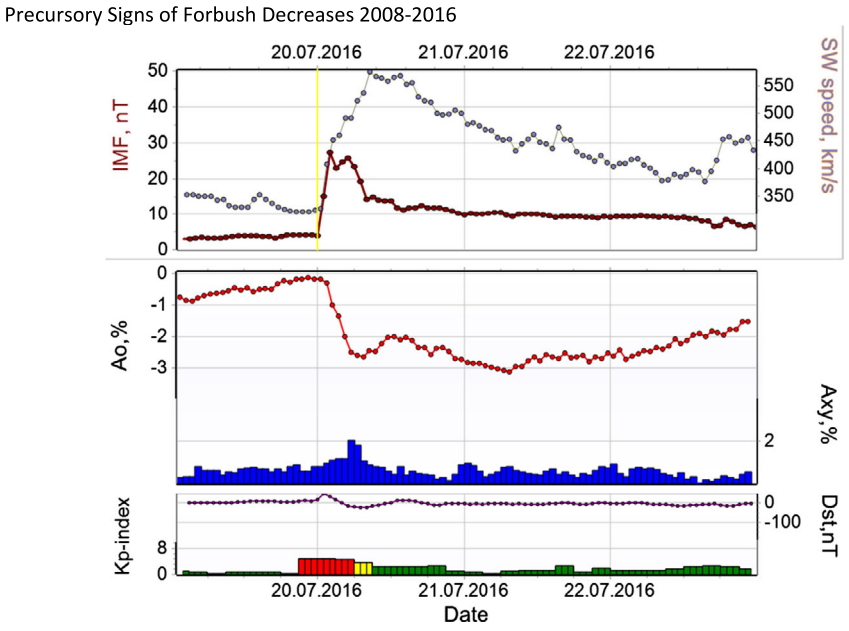

Figure 5 Time profiles of the solar wind velocity (*purple line*) and the interplanetary magnetic field (*red line*) (*upper panel*), of the CR density (A_0) (*red line*) and the anisotropy on the ecliptic plane A_{xy} (*blue histogram*) (*middle panel*) and of the geomagnetic indices Dst and Kp (*line* and *histogram*, respectively) (*lower panel*) for the FD on 19 July 2016.

between 70° – 190°, mostly from 100° to 180° (Lingri *et al.*, 2016b). The time period of the precursor observations differs from event to event and it could last from 18 h to 4 h before the start of the FD depending on the situation in the heliosphere, and during the last hours the effect increases. Most of the events have sources located in the center of the solar disc or slightly shifted to the east.

3.2. Forbush Decreases with Pre-increase Precursors

The second group is composed of FDs characterized by only pre-increase signs before the SSC. Five events: 12 March 2012; 23 June 2013; 07 January 2014; 06 November 2015 and 19 July 2016 belong to this category. They were associated with central or eastern solar sources (Table 1), as it has been already mentioned in previous work (*e.g.* Papailiou *et al.*, 2012a).

We will focus in one interesting FD of this group that occurred on 19 July 2016 at 23:51 UT. The active region AR 12567, on the central region of the solar disc, was on the rise and provided solar flares at that time period. A halo CME had velocity of 340 km s^{-1}. The interplanetary parameters, disturbed by the solar wind, managed to reach the velocity of 576 km s^{-1} and the IMF to reach the high value of 27.3 nT soon after the shock's arrival (Figure 5, upper panel). The CR intensity at the rigidity of 10 GV decreased by 2.9%, and the A_{xy} anisotropy increased up to $\approx 2\%$ (Figure 5, middle panel). The geomagnetic indices Kp and Dst changed slightly and reached the values of 5 and -23 nT, respectively (Figure 5, lower panel). The north–south component of the CR anisotropy changed in direction and increased significantly ($A_z = 2.7\%$) (Figure 6).

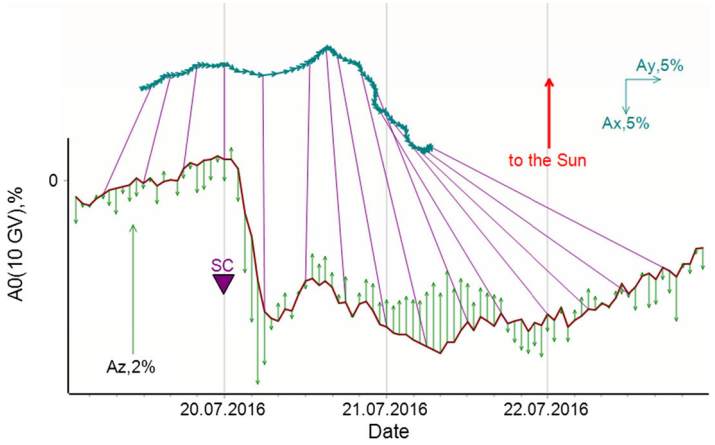

Figure 6 The anisotropy variation on the ecliptic plane (A_{xy} – *blue vectors*) and of the z component (A_z – *green vectors*) during the time period of the event of 19 July 2016. The *red line* represents the A_0 component. *Purple lines* connect the same points in time on two curves.

If we examine the asymptotic longitude diagram of this event, pre-increase signs are obvious in this FD, which are sketched with the yellow dots on Figure 7 (upper panel). The red dots continue to present the main FD. The precursor began about 10 h before the shock's arrival and was observed in a specific asymptotic longitude range from 230° to 300°. Pre-increase started in a narrower longitudinal range (250° – 290°), and then extended to a wider longitudinal range continuing after the shock wave's arrival. The dependence of the CR variation on the NMs asymptotic longitudes is typical with maximal variations in 150° – 270° (Figure 7, lower panel). In Figure 7 (lower panel) a significant increase in the amplitude of the CR anisotropy is depicted. The minimum of the CR variations is explicitly pronounced in the range of 110° – 160°. In general, the longitudinal distribution does not contradict the distribution for the first spherical harmonic.

There is also a common region of asymptotic longitudes in this category, where the pre-increase existed, ranging from 190° to 300°. The time period that the pre-increase precursor was observed in our data started in average 10 – 14 h before the SSC and was maintained until the FD's start. Sources of events are widely distributed in longitude.

3.3. Forbush Decreases with Pre-decrease and Pre-increase Precursors

The last group includes FDs that are associated with both pre-decrease and pre-increase precursor signs. Pre-increase appeared first and after a time delay of 6 to 10 h a pre-decrease sign was observed. It is noted that six FDs exist in this category: 10 March 2011; 24 October 2011; 14 July 2012; 15 February 2014; 07 June 2014 and 31 December 2015. The solar sources of these events were located in the central and the eastern regions of the solar disc.

The event which occurred on 14 July 2012 at 18:09 UT is used as an example in this category. Many other studies have already analyzed this specific event from other points of view (*e.g.* Lingri *et al.*, 2016a; Kuai *et al.*, 2017). It was associated with a halo CME with a velocity of 885 km s^{-1}. The solar wind velocity increased rapidly and reached the value of 667 km s^{-1} and also, in the same way, the IMF reacted and achieved the value of 27.3 nT (Figure 8, upper panel). The produced FD was of two steps and its amplitude

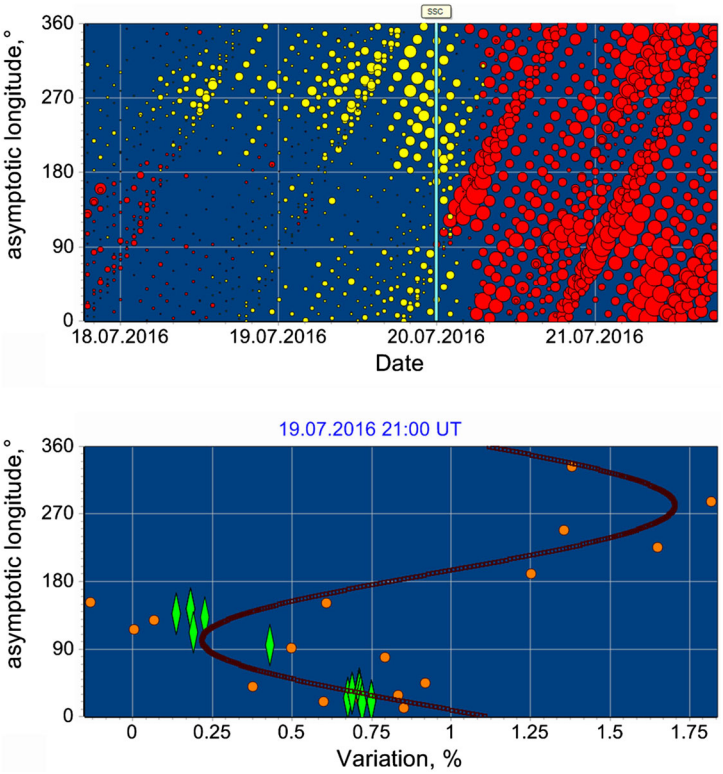

Figure 7 The asymptotic longitude of each station *versus* the date (*upper panel*) of the FD of 19 July 2016. The *red circles* represent decrease in the CR intensity while *yellow* ones represent increase. *Cyan vertical line* is the shock's arrival time. The switching of *yellow* and *red circles* two days before the FD is the solar diurnal anisotropy record. The size of its bubble is proportional to the recorded amplitude of each station every hour. The asymptotic longitude of each station *versus* hourly cosmic ray variations of NMs (*lower panel*) at 21:00 UT on 19 July 2016 (1 h before the FD's onset) is presented. The *orange dots* present the hourly CR variations, the *green diamonds* present CR variations averaged within the sector $\pm 20°$ and the *curve* gives the fitting of the first harmonic of the anisotropy (solar–diurnal variation) calculated from the longitudinal distribution.

reached the value of 6.4% for cosmic rays of 10 GV rigidity and significant changes of the A_{xy} component took place (Figure 8, middle panel). A strong geomagnetic storm was also recorded with the Dst index reaching the minimum value of −133 nT (Figure 8, lower panel).

The A_{xy} and A_z components of the anisotropy increased as the SSC and A_{xy} changed its direction significantly (about 60°) after the arrival of the main ejecta ($A_{xy} = 2.62\%$, $A_z = 2.73\%$) (Figure 9). A pre-increase precursor was observed 10 h before the FD at an asymptotic longitude range between 180° and 330°, which is shown in Figure 10 (upper panel). In the meantime a pre-decrease sign started to be recorded by the NMs worldwide network about 4 h before the SSC in a range of 60° – 130°. As it is depicted in the lower panel of Figure 10, 2 h before the shock arrival, it demonstrated increasing variations with maximal values in 170° – 330°. This distribution is similar to a sine wave, but enhanced. Many stations show a significant increase in variations and a few stations present a deep minimum. It is important to note that the amplitude increased significantly (by 2 – 3 times).

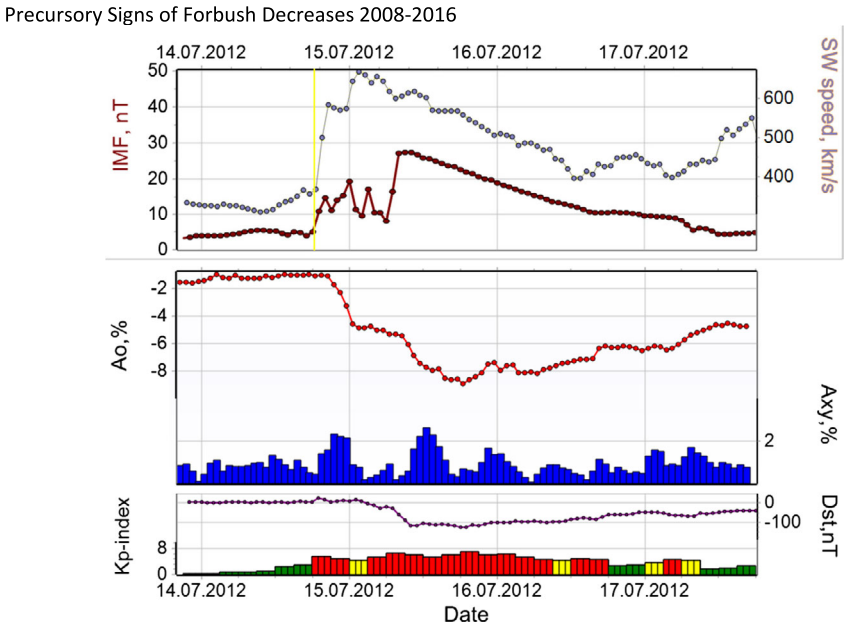

Figure 8 Time profiles of the solar wind velocity (*purple line*) and the interplanetary magnetic field (*red line*) (*upper panel*), of the CR density (A_0) (*red line*) and the anisotropy on the ecliptic plane A_{xy} (*blue histogram*) (*middle panel*) and of the geomagnetic indices Dst and Kp (*line* and *histogram*, respectively) (*lower panel*) for the FD on 14 July 2012.

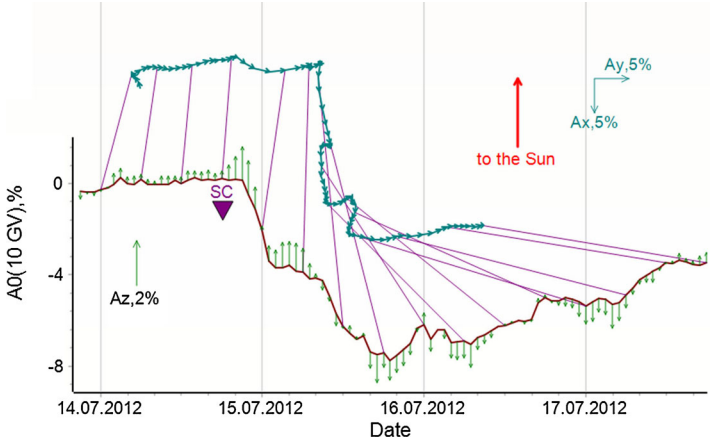

Figure 9 The anisotropy variation on the ecliptic plane (A_{xy} – *blue vectors*) and of the z component (A_z – *green vectors*) during the time period of the event of 14 July 2016. The *red line* represents the A_0 component. *Purple lines* connect the same points in time on two curves.

At longitudes of pre-decrease (60° – 130°), the FD begins immediately, but at longitudes with pre-increase (180° – 330°), the onset is delayed by 3 – 4 h.

To sum up, in this group both FD precursors are recorded with the pre-increase of the cosmic ray intensity to be identified in about 6 – 12 h and the pre-decrease in 2 – 3 h be-

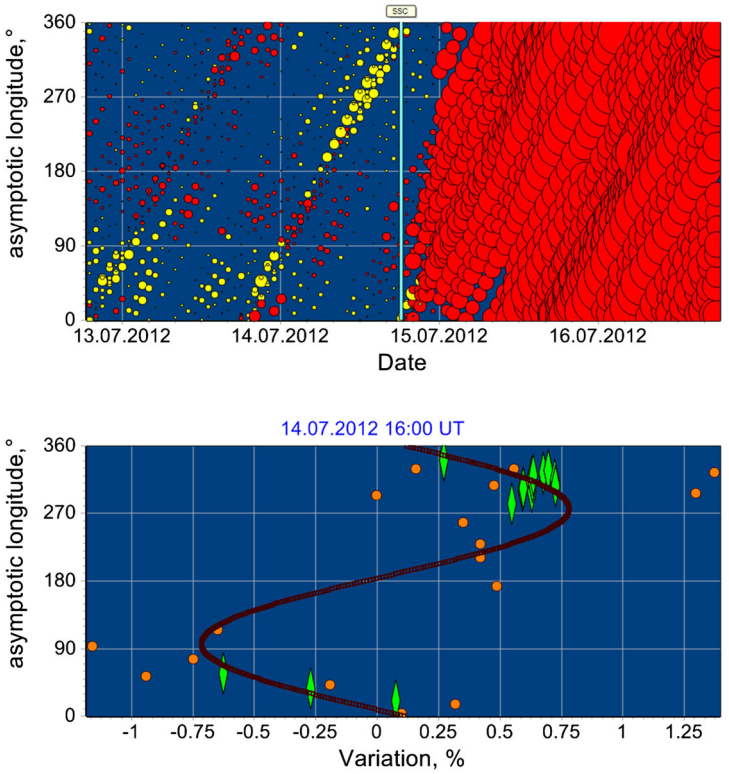

Figure 10 The asymptotic longitude of each station *versus* the date (*upper panel*) of the FD on 14 July 2012. The *red circles* represent decrease in the CR intensity while *yellow* ones represent increase. *Cyan vertical line* is the shock's arrival time. The switching of *yellow* and *red circles* two days before the FD is the solar diurnal anisotropy record. The size of its bubble is proportional to the recorded amplitude of each station every hour. The asymptotic longitude of each station versus hourly cosmic ray variations of NMs (*lower panel*) at 16:00 UT on 14 July 2012 (1 h before the FD's onset) is presented. The *orange dots* present the hourly CR variations, the *green diamonds* present CR variations averaged within the sector $\pm 20°$ and the *curve* gives the fitting of the first harmonic of the anisotropy (solar–diurnal variation) calculated from the longitudinal distribution.

fore the SSC, as it is presented in Figure 10. This is due to the magnetic connection of the Earth's magnetosphere and the loss cone region (Nagashima *et al.*, 1993; Belov *et al.*, 1995; Asipenka *et al.*, 2009). The ranges of the asymptotic longitude of both precursors are different: with the pre-decrease ranging from 0° to 150° in average, while the pre-increase is observed within the range of 180° to 330°. Only in the event of 07 June 2014 the pre-decrease starts long before the shock wave (about 22 h), and the pre-increase begins 12 h before the main phase of the FD. This suggests that the pre-decrease of the FD can have a longer duration and begins even before the pre-increase.

4. Discussion and Conclusions

In this work, FD events of cosmic ray intensity associated with the existence of SSC were studied. This is really crucial because when a FD is associated with a SSC, it means that it

is connected with a solar source which, in the most cases is an ICME. It is helpful to study the CR intensity variations before the main phase of the FD and to categorize it according to their sources' characteristics. Specifically from a total of 1010 events referred in the FEID during the examined period from 2008 to 2016, 164 were associated with a SSC and a percentage of 70% of them were connected with an ICME. It is an important point for the Space Weather research.

The main conclusions of this research are summarized now:

i) Although the current Solar Cycle 24 was not an active one, 142 FDs with amplitude greater than 2% were observed during this time period. Based on the two main adopted criteria of this study; FD size, which is used for first time in the FD precursors study, and SSC existence, 62 events were selected to be investigated for precursor signs.

ii) In addition to the above conditions, the CR density and anisotropy in the ecliptic plane, 1 h before the SSC is another adopted criterion in this analysis and the value of the A_{xy} component is chosen to be greater than 0.8%, instead of 1.2% as previous studies, after a detailed analysis of all events. We recall here that the mean anisotropy value of the CR anisotropy A_{xy} is about 0.51 – 0.53% (Belov *et al.*, 2017a). In previous articles, the CR anisotropy was taken as the main and unique criterion of investigation for FD precursors. In that case the value of the anisotropy variation of $> 1.2\%$ was considered satisfying. In this study the anisotropy value was considered to be higher than the value of 0.8%, as more FDs events with precursory signals could be investigated. This new value of the anisotropy limits the examined FDs to 34 and among them 16 events presented precursory signals. This means that a percentage of 47% of these events were revealed with observable precursors, instead of $\approx 30\%$ appeared in previous studies (*e.g.* Papailiou *et al.*, 2012a).

iii) The outlined precursory sings in this study were distinguished into three categories: pre-decreases only, pre-increases only and both pre-decreases and pre-increases precursors. This last category is noticeable for the first time. The timestamp of the precursor before the start of the FD depends on the Earth's position relatively to the upcoming disturbances, on the different nature of the solar ejection and on the interplanetary conditions in the examined time period.

iv) Most of the events with precursors under investigation were associated with solar sources from the central part of the Sun. In this work we cannot confirm if the precursor events were mainly connected with western or eastern sources and a definite conclusion could not be outlined. It is noted that in our case the total of the 16 events that revealed precursory signals were associated with CME, as it appears in Table 1.

v) From the study of the asymptotic longitude-time diagrams and the asymptotic longitude-variation ones it is concluded that the asymptotic longitudes where a precursory signal was observed as well as the time ranges they could be seen, are different among the three categories of the events. In average, the pre-decreases of the cosmic ray intensity are observed in asymptotic longitudes ranged at $\approx 70^\circ - 190^\circ$ in about 18 h before the SSC, while the pre-increases in a range of $\approx 190^\circ - 300^\circ$ in about 10 h before the start of the event. This is in agreement with previous results (Asipenka *et al.*, 2009; Papailiou *et al.*, 2012a).

vi) In the case of the events with both signals, pre-decreases and pre-increases, it was shown that the asymptotic longitude range varies from $\approx 180^\circ - 330^\circ$ for the pre-increases and from $\approx 0^\circ - 150^\circ$ for the pre-decreases, with the pre-increases to be observed at first and the pre-decrease signals to follow at a time interval of 4 to 10 h. In most cases (five to six events), the pre-increase begins 6 – 12 h before the arrival of the shock wave, and the pre-decrease begins only 2 – 3 h before the start of the event. These asymptotic ranges in this category are wider than those of the events with only one signal. In this case, the duration of

the pre-decrease signal is considerably smaller than the one of the first category. This result has not been observed again and a further investigation for similar precursors in previous Solar Cycles is required.

When the pre-increase appears, very often the increase in CR intensity continues beyond the shock wave that leads to a later start of the FD, as it was observed at some stations. A pre-decrease is a clear anisotropic effect, which is often observed in a narrower longitude range, and the pre-increase is observed in a much broader longitude range and usually has an isotropic component.

vii) The mean value of the maximum velocity of the solar wind in the three categories discussed above is quite similar. For the FDs that are associated with pre-decreases the velocity is 533 km s^{-1} for the interplanetary space, while for the FDs belonging to the other two categories is 569 km s^{-1}. Comparing this value to the background velocity of the three categories, it is evident that the differences are of the same order, with the greatest difference appearing in the pre-decrease category and reaching the value of 82 km s^{-1}. Thus, we do not find a connection of the precursor type with the maximum velocity of the interplanetary disturbance and/or with the difference of this velocity with the background velocity of the solar wind.

Summarizing, it is noted that the first harmonic of the CR anisotropy increases significantly some hours before the SSC, which is really helpful in forecasting the upcoming disturbance. It must also be noticed that during the FDs, the individual solar, interplanetary and geomagnetic parameters increase, and in some cases not analogically. The general remarks and the new adopted criteria presented in this article will soon be applied to the whole time period of the neutron monitors operation. This work is a reviewing and update of this specific research on the FD precursors aiming to be useful for the FD monitoring and forecasting in real time, one of the main goals of the European Space Weather Agency. This work confirms once again that these phenomena appear often enough and the available ground level CR detectors permit us to distinguish and research FD precursors.

Finally, we would like to mention that except of these events associated with SSC, there are FDs that even though they are not connected with SSCs, warning signs before the main phase of the event are also observed. These FDs are not often and their amplitudes are in average smaller than those of the FDs with SSC. These FDs will be analyzed in a future work.

Acknowledgements This research work was supported by the Hellenic Foundation for Research and Innovation (HFRI) and the General Secretariat for Research and Technology (GSRT), under the HFRI PhD Fellowship grant (GA. no. 14492) and was partly supported by the RFBR grant 18-02-00451a and by the Russian Science Foundation under grant 19-72-20083. Special thanks to the colleagues of the NM stations (www.nmdb.eu) for kindly providing the cosmic ray data used in this study in the frame of the High resolution Neutron Monitor database NMDB funded under the European Union's FP7 Program (contract no. 213007). Works were performed using the equipment of the USU "CR Network". Thanks are due to the IZMIRAN/FEID, ACE/Wind, OMNI and NOAA data centers.

Disclosure of Potential Conflicts of Interest The authors declare that they have no conflicts of interest.

References

Abunin, A.A., Abunina, M.A., Belov, A.V., Eroshenko, E.A., Oleneva, V.A., Yanke, V.G.: 2012, Forbush effects with a sudden and gradual onset. *Geomagn. Aeron.* **52**, 292. DOI.

Asipenka, A.S., Belov, A.V., Eroshenko, E.A., Klepach, E.G., Oleneva, V.A., Yanke, V.G.: 2009, Interactive database of cosmic ray anisotropy (DB-A10). *Adv. Space Res.* **43**, 708. DOI.

Aslam, O.P.M., Badruddin: 2017, Study of the geoeffectiveness and galactic cosmic-ray response of VarSITI-ISEST campaign events in Solar Cycle 24. *Solar Phys.* **292**, 135. DOI.

Belov, A.V.: 2009, Forbush effects and their connection with solar, interplanetary and geomagnetic phenomena. In: Gopalswamy, N., Webb, D.F. (eds.) *Universal Heliophysical Processes*, *Proc. IAU Symp.* **257**, Cambridge University Press, Cambridge, 439. DOI.

Belov, A.V., Dorman, L.I., Eroshenko, E.A., Iucci, N., Villoresi, G., Yanke, V.G.: 1995, Search for predictors of Forbush decreases. In: Iucci, N., Lamanna, E. (eds.) *Proc. 24th ICRC, Rome*, **4**, 888.

Belov, A.V., Bieber, J.W., Eroshenko, E.A., Evenson, P., Pyle, R., Yanke, V.G.: 2003, Cosmic ray anisotropy before and during the passage of major solar wind disturbances. *Adv. Space Res.* **31**, 919. DOI.

Belov, A., Abunin, A., Abunina, M., Eroshenko, E., Oleneva, V., Yanke, V., Papaioannou, A., Mavromichalaki, H., Gopalswamy, N., Yashiro, S.: 2014, Coronal mass ejections and non-recurrent Forbush decreases. *Solar Phys.* **289**, 3949. DOI.

Belov, A.V., Abunina, M.A., Abunin, A.A., Eroshenko, E.A., Oleneva, V.A., Yanke, V.G.: 2017a, Cosmic-ray vector anisotropy and local characteristics of the interplanetary medium. *Geomagn. Aeron.* **57**, 389. DOI.

Belov, A.V., Abunina, M.A., Abunin, A.A., Eroshenko, E.A., Oleneva, V.A., Yanke, V.G.: 2017b, Vector anisotropy of cosmic rays in the beginning of Forbush effects. *Geomagn. Aeron.* **57**, 541. DOI.

Belov, A., Eroshenko, E., Yanke, V., Oleneva, V., Abunin, A., Abunina, M., Papaioannou, A., Mavromichalaki, H.: 2018, The global survey method applied to ground-level cosmic ray measurements. *Solar Phys.* **293**, 68. DOI.

Cane, H.V.: 2000, Coronal mass ejections and Forbush decreases. *Space Sci. Rev.* **93**, 55. DOI.

Dorman, L.I., Villoresi, G., Belov, A.V., Eroshenko, E.A., Iucci, N., Yanke, V.G., Yudakhin, K.F., Bavassano, B., Ptitsyna, N.G., Tyasto, M.I.: 1995, Cosmic-ray forecasting features for big Forbush decreases. *Nucl. Phys. B, Proc. Suppl.* **39**, 136. DOI.

Dumbovic, M., Vrsnak, B., Calogovic, J., Zupan, R.: 2012, Cosmic ray modulation by different types of solar wind disturbances. *Astron. Astrophys.* **538**, A28. DOI.

Forbush, S.E.: 1954, World-wide cosmic-ray variations, 1937 – 1952. *J. Geophys. Res.* **59**, 525. DOI.

Fushishita, A., Kuwabara, T., Kato, C., Yasue, S., Bieber, J.W., Evenson, P., Da Silva, M.R., Dal Lago, A., Schuch, N.J., Tokumaru, M., Duldig, M.L., Humble, J.E., Sabbah, I., Jassar, H.K.A., Sharma, M.M., Munakata, K.: 2010, Precursors of the Forbush decrease on 2006 December 14 observed with the Global Muon Detector Network (GMDN). *Astrophys. J.* **715**, 1239. DOI.

Gerontidou, M., Mavromichalaki, H., Daglis, T.: 2018, High-speed solar wind streams and geomagnetic storms during Solar Cycle 24. *Solar Phys.* **293**, 131. DOI.

Gopalswamy, N., Lara, A., Yashiro, S., Kaiser, M.L., Howard, R.A.: 2001, Predicting the 1-AU arrival times of coronal mass ejections. *J. Geophys. Res.* **106**, 207. DOI.

Kozai, M., Munakata, K., Kato, C., Kuwabara, T., Rockenabach, M., Dal Lago, A., Schuch, N.J., Braga, C.R., Mendonça, R.R.S., Al Jassar, H.K., Sharma, M.M., Duldig, M.L., Humble, J.E., Evenson, P., Sabbah, I., Tokumaru, M.: 2016, Average spatial distribution of cosmic rays behind the interplanetary shock – Global Muon Detector Network observations. *Astrophys. J.* **825**, 100. DOI.

Kuai, J., Liu, L., Lei, J., Liu, J., Zhao, B., Chen, Y., Le, H., Wang, Y., Hu, L.: 2017, Regional differences of the ionospheric response to the July 2012 geomagnetic storm. *J. Geophys. Res.* **122**, 4654. DOI.

Leerungnavarat, K., Ruffolo, D., Bieber, J.W.: 2003, Loss cone precursors to Forbush decreases and advance warning of space weather effects. *Astrophys. J.* **593**, 587. DOI.

Lingri, D., Mavromichalaki, H., Belov, A., Eroshenko, E., Yanke, V., Abunin, A., Abunina, M.: 2016a, Solar activity parameters and associated Forbush decreases during the minimum between Cycles 23 and 24 and the ascending phase of Cycle 24. *Solar Phys.* **291**, 1025. DOI.

Lingri, D., Mavromichalaki, H., Belov, A., Erosenko, E., Yanke, V., Abunin, A., Abunina, M.: 2016b, Forbush decreases during the DeepMin and MiniMax of Solar Cycle 24. In: *XXV ECRS 2016 Proceedings – eConf C16-09-04.3*. arXiv.

Lockwood, J.A.: 1971, Forbush decreases in the cosmic radiation. *Space Sci. Rev.* **12**, 658. DOI.

Mavromichalaki, H., Papaioannou, A., Petrides, A., Assimakopoulos, B., Sarlanis, C., Souvatzoglou, G.: 2005, Cosmic ray events related to solar activity recorded at the Athens Neutron Monitor Station for the period 2000 – 2003. *Int. J. Mod. Phys. A* **20**, 6714. DOI.

Mavromichalaki, H., Papaioannou, A., Plainaki, C., Sarlanis, C., Souvatzoglou, G., Gerontidou, M., Papailiou, M., Eroshenko, E., Belov, A., Yanke, V., Flückiger, E.O., Bütikofer, R., Parisi, M., Storini, M., Klein, K.-L., Fuller, N., Steigies, C.T., Rother, O.M., Heber, B., Wimmer-Schweingruber, R.F., Kudela, K., Strharsky, I., Langer, R., Usoskin, I., Ibragimov, A., Chilingaryan, A., Hovsepyan, G., Reymers, A., Yeghikyan, A., Kryakunova, O., Dryn, E., Nikolayevskiy, N., Dorman, L., Pustil'nik, L.: 2011, Applications and usage of the real-time Neutron Monitor Database. *Adv. Space Res.* **47**, 2210. DOI.

Melkumyan, A.A., Belov, A.V., Abunina, M.A., Abunin, A.A., Eroshenko, E.A., Yanke, V.G., Oleneva, V.A.: 2019, Comparison between statistical properties of Forbush decreases caused by solar wind disturbances from coronal mass ejections and coronal holes. *Adv. Space Res.* **63**(2), 1100. DOI.

Munakata, K., Kuwabara, T., Yasue, S., Kato, C., Akahane, S., Koyama, M., Ohashi, Y., Okada, A., Aoki, T., Mitsui, K., Kojima, H., Bieber, J.W.: 2005, A "loss cone" precursor of an approaching shock observed by a cosmic ray muon hodoscope on October 28, 2003. *Geophys. Res. Lett.* **32**, L03S04. DOI.

Nagashima, K., Sakakibara, S., Fujimoto, K., Fujji, Z., Ueno, H.: 1993, Local-time-dependent precursory decrease of cosmic rays, in front of Forbush-decrease-associated IMF shock wave, observed on September 9, 1992. In: Leahy, D.A., Hickws, R.B., Venkatesan, D. (eds.) *Proc. 23rd ICRC, Invited, Rapporteur, and Highlight Papers*, *Calgary, Canada* **3**, World Scientific, Singapore, 711.

Paouris, E., Mavromichalaki, H.: 2017, Interplanetary coronal mass ejections resulting from Earth-directed CMEs using SOHO and ACE combined data during Solar Cycle 23. *Solar Phys.* **292**, 30. DOI.

Papailiou, M., Mavromichalaki, H., Belov, A., Eroshenko, E., Yanke, V.: 2012a, Precursor effects in different cases of Forbush decreases. *Solar Phys.* **276**, 337. DOI.

Papailiou, M., Mavromichalaki, H., Belov, A., Eroshenko, E., Yanke, V.: 2012b, The asymptotic longitudinal cosmic ray intensity distribution as a precursor of Forbush decreases. *Solar Phys.* **280**, 641. DOI.

Plainaki, C., Mavromichalaki, H., Belov, A., Eroshenko, E., Yanke, V.: 2009, Neutron monitor asymptotic directions of viewing during the event of 13 December 2006. *Adv. Space Res.* **43**, 518. DOI.

Ross, E., Chaplin, W.: 2019, The behaviour of galactic cosmic-ray intensity during solar activity Cycle 24. *Solar Phys.* **294**, 8. DOI.

Tortermpun, U., Ruffolo, D., Bieber, J.W.: 2018, Galactic cosmic-ray anistropy during the Forbush decrease starting 2013 April 13. *Astrophys. J.* **852**, L26. DOI.

Tsyganenko, N., Stern, D.: 1996, Modeling the global magnetic field of the large-scale Birkeland current systems. *J. Geophys. Res.* **101**, 27187. DOI.